arXiv:1702.07110v1 [cond-mat.mes-hall] 23 Feb 2017

Synchronized magnon-photon coupling

Vahram L. Grigoryan[1] and Ke Xia[1,2,*]

[1]*The Center for Advanced Quantum Studies and Department of Physics, Beijing Normal University, Beijing 100875, China*
[2]*Synergetic Innovation Center for Quantum Effects and Applications (SICQEA), Hunan Normal University, Changsha 410081, China*

We study magnon-photon coupling in cavity in the presence of relative phase shift between magnetic and electric components of the microwave. We show that the anticrossing gap can be manipulated by varying the relative phase. Increasing the phase difference leads to narrowing the anticrossing gap of hybridized modes and eventually to phase locked coupling at the value of relative phase close to π. The FMR and cavity modes become phase locked and oscillate at almost the same frequency near the resonance frequency. Characteristic linewidth drop and transmission amplitude enhancement are demonstrated. The phase resolved magnon-photon coupling can be used both for phase imaging and controlling coupling parameters.

Strong light-matter interactions in condensed matter systems are a rich source of physics. It seeks ways to expand our ability to use light for many purposes: to observe and manipulate matter at the atomic scale, to use nanostructures to manipulate light at the subwavelength scale, as well as to explore such important concepts as the polariton [1] aiming to develop quantum information technology. After reaching a regime of dramatically enhanced coupling by exploiting cooperative phenomena in spin ensembles [2, 3] much work has been devoted to the strong magnon-photon interactions between low loss magnetic materials and high quality microwave cavities [4–12]. Coherent coupling between single spin and microwave cavity photons [13], ferromagnetic magnon and a superconducting qubit [14] as well as cavity photons and magnons in magnetic materials [9–12] has been reported. Cavity mediated indirect coupling between spin-like objects have been demonstrated in the context of cavity [15] and circuit quantum electrodynamics [16, 17]. In addition to widely used microwave transmission measurements of magnon-photon coupling at room temperature, electrical detection method has been recently demostrated by Hu's group [18]. Theoretically, the magnon-polariton coupling has been formulated by means of scattering theory by Cao *et. al.* [19] as well as simple semiclassical model by Hu's group [18]. The relevance of the classical picture to quantum mechanical picture has been discussed elsewhere [20]. Characteristic coupling features such as ferromagnetic resonance (FMR) modes anticrossing in case of microwave transmission measurements and asymmetric FMR-like modes for electrically detected technique has been demonstrated. However, it is shown that although the intrinsic Gilbert damping is not changed by the coupling, the linewidth always increases drastically as the FMR approaches the resonant coupling condition.

To overcome the drawback of wide linewidth while having strong magnon-photon coupling we consider magnon photon coupling in cavity resonator when a relative phase shift (Φ) between electric and magnetic components of microwave is introduced. The physics of Φ is in principle contained in Maxwell's equations. However, due to the technical problems for simultaneously and coherently probing both electric and magnetic fields, the effect of the relative phase has not been considered until the development of spintronic Michelson interferometry [21]. The microwave signal in this device is split into two coherent beams by microwave power divider. One of the beams then travels through a microwave phase shifter before arriving to a sensor. The other beam travels directly to the sensor through a coaxial cable. This effectively creates four time-dependent signals (two magnetic fields and two electric fields). This makes possible for the dominant electric and magnetic fields within the sensor come from different beams and thus to control the relative phase between electric and magnetic fields due to a phase shifter in one of the pathes [21–24]. This technique opens a new perspectives in study of interaction of spin and light.

In this letter we study theoretically the coupling of magnons with electromagnetic wave with relative phase difference between microwave electric and magnetic components. Proper experimental design allowing to generate relative phase shifted microwave in a cavity will reveal new features of magnon-polariton coupling. We show that for magnon-photon coupling the relative phase (Φ) between the microwave electric and magnetic fields plays the leading role in the FMR line shape. The spectrum of hybridized modes depends on the relative phase Φ. Particularly, the gap between two modes of polariton close to the resonance frequencies can be tuned by varying Φ. More interestingly, phase locked coupling regime can be achieved by tuning the relative phase close to π. Important consequence of the phase locked coupling is that together with achievement of strongly coupled modes the linewidth, at the same time, becomes very narrow with enhanced output microwave power. The phase resolved magnon photon coupling can be used both for phase imaging and controlling coupling parameters.

Simple semiclassical picture describing magnon-phonon interaction in the cavity is based on combination of a microwave LCR and Landau-Lifshitz-Gilbert (LLG) equations [18, 25]. In the presence of the microwave with magnon-photon coupling, two classical coupling mechanisms of magnetization dynamics with electromagnetic wave play role. First one is known as the Faraday induction of FMR [26] which induces voltage in LCR circuit due to the precessing magnetization. The other coupling mechanism is governed by Ampere's law producing magnetic field (that is the magnetic

component of microwave).

The RLC circuit equation of two crossed coils parallel to the $\hat{\mathbf{x}}$ and $\hat{\mathbf{y}}$ directions, in which the microwave current $\mathbf{j}(t)$ is driven by the RF voltage $\mathbf{V}$ is

$$L\dot{\mathbf{j}} + R\mathbf{j} + (1/C)\int \mathbf{j}dt = \mathbf{V}, \tag{1}$$

where L, C, and R are inductor, capacitor, and resistor, respectively. The driving voltage $\mathbf{V} = \mathbf{V}_{app} + \mathbf{V}^F$, where $\mathbf{V}_{app} = (V_{app,x}, V_{app,y}, 0)$ is the applied voltage and $\mathbf{V}^F$ is induced from precessing magnetization according to Faraday induction

$$V_x^F(t) = K_c L\dot{m}_y,\ V_y^F(t) = -K_c L\dot{m}_x, \tag{2}$$

The magnetization precession in the magnetic sample is governed by the LLG equation [27]

$$\dot{\mathbf{m}} = \mathbf{m}\times\gamma\mathbf{H} - \alpha\mathbf{m}\times\dot{\mathbf{m}}, \tag{3}$$

where $\mathbf{m} = \mathbf{M}/M_s$ is the magnetization direction in FM with M_s being the saturation magnetization. α is the intrinsic Gilbert damping parameter. $\mathbf{H} = \mathbf{H}_0 + \mathbf{h}^A$ is the effective magnetic field in FM with $\mathbf{H}_0 = H_0\hat{\mathbf{z}}$ being external magnetic field applied in $\hat{\mathbf{z}}$ direction. $\mathbf{h}^A = \mathbf{h}e^{-i(\omega t-\Phi)}$ is phase shifted magnetic field of microwave with Φ being the relative phase between electric and magnetic components of microwave [**?**]. Using the form of magnetization $\mathbf{m} = \hat{\mathbf{z}} + \mathbf{m}_\perp e^{-i\omega t}$ the linearized LLG equation becomes

$$m^+(\omega - \omega_r + i\alpha\omega) + e^{i\Phi}\omega_m h^+ = 0, \tag{4}$$

where $m^+ = m_x + im_y$ is in-plane component of the magnetization, $\omega_m = \gamma M_s$ with γ being the gyromagnetic ratio, $h^+ = h_x + ih_y$, due to the Ampere's law

$$h_x = K_m j_y,\ h_y = -K_m j_x \tag{5}$$

which places a torque on the FM magnetization. Here $j_{x,y}$ are the current components in the circuit, satisfying Eq. (1). Parameters K_c and K_m are coupling parameters. The linearized equations of motion solved by the form $\mathbf{j} = \mathbf{j}_\perp e^{i\omega t}$ leads to

$$\Omega\begin{pmatrix} m^+ \\ h^+ \end{pmatrix} = 0 \quad \text{with}$$
$$\Omega \equiv \begin{pmatrix} \omega - \omega_r + i\alpha\omega & \omega_m e^{i\Phi} \\ \omega^2 K^2 & \omega^2 + 2i\beta\omega\omega_c - \omega_c^2 \end{pmatrix} \tag{6}$$

where $K \simeq \sqrt{K_c K_m}$, $\omega_r \simeq \gamma H_0$, the cavity frequency is $\omega_c = 1/\sqrt{LC}$, and $\beta = R/2L\omega_c$ is the cavity mode damping.

By solving the complex eigenfrequencies of Eq. (6) ($\det\Omega = 0$) at given magnetic field we obtain two roots for ω. The real components of ω determine resonant frequencies, while imaginary part describes damping of the coupled system. In Fig. 1 we plot the dispersion spectrum $\mathrm{Re}\,(\omega(\omega_r))$

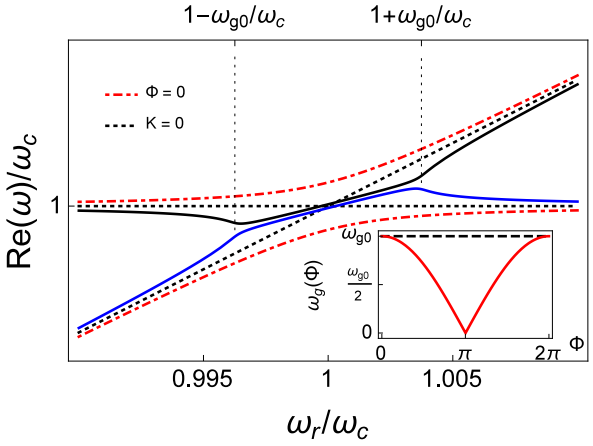

Figure 1. (Color online) Dispersion relation of FM coupled to microwave mode for different values of relative phase Φ. Solid, dash-dotted and dotted curves correspond to $\Phi \approx \pi$, $\Phi = 0$ and $K = 0$, respectively. Dotted curve represents the FMR and cavity modes in the absence of coupling. The inset shows evolution of ω_g gap between modes as a function of the phase shift at $\omega_r = \omega_c$.

(normalized by ω_c) for different values of relative phase Φ. Dotted lines correspond to cavity mode and the Kittel's mode in the absence of magnon-photon coupling. For symmetry of the system we set equal damping for FMR and LCR as $\alpha = \beta = 0.002$, $\omega_m = \gamma M_s \approx 0.075\omega_c$, the coupling parameter is $K = 0.01$ [28], with $\omega_c/2\pi \approx 10.5$ GHz.

For $\Phi = 0$ (dash-dotted lines in Fig. 1) we have the characteristic anticrossing of two modes [18] where the gap between two modes at FMR resonance ($\omega_r = \omega_c$) is proportional to the coupling constant K and can be approximated as $\omega_{g0} \equiv \omega_g(\Phi = 0) = K\sqrt{2\omega_m\omega_c}$ [28]. However, as shown in the inset of Fig. 1, tuning the relative phase changes the gap between two modes at FMR resonance. The relative phase shift causes principally different picture of spin-photon coupling spectrum as well as the transmission amplitude. Comparison of spectra for $\Phi = 0$ and $\Phi \approx \pi$ in Fig. 1 shows that the relative phase shift between electric and magnetic components of microwave switches the order of energy transfer between FMR and microwave modes. For $\Phi = 0$ at $\omega_r < \omega_c$ the frequency of FMR mode decreases with increasing frequency of cavity mode and the opposite at $\omega_r > \omega_c$. The picture is now inverse at $\Phi = \pi$: due to the phase shift now the FMR mode frequency increases at $\omega_r < \omega_c$ together with decreasing of cavity mode frequency and the opposite at $\omega_r > \omega_c$. As a consequence a gap is opened due to the coupling in $\Phi = 0$ case while increasing Φ eventually leads to phase locked synchronization of two modes at $\Phi \approx \pi$ when two modes start to beat at almost the same frequency equals to $(\omega_c + \omega_r)/2$. In the presence of phase shift the dependence of gap on Φ at $\omega_r = \omega_c$ can be approximated as $\omega_g(\Phi) = K\sqrt{2\omega_m\omega_c}\,|\cos(\Phi/2)|$.

Synchronization of coupled oscillators, generally referred to as injection locking, phase locking or frequency entrainment, has numerous examples in nature and generally occurs

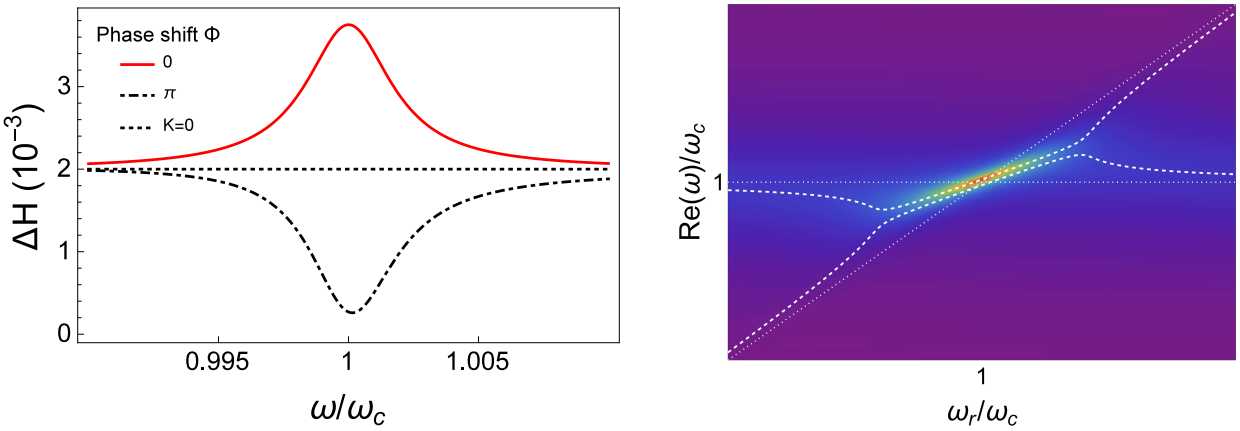

Figure 2. (Color online) (a) Normalized FMR linewidth ΔH as a function of ω for the values of relative phase shift $\Phi = 0$ (solid line) and $\Phi \approx \pi$ (dash-dotted line). The dashed line shows the linewidth in the absence of magnon-photon coupling. (b) Dispersion relation of coupled (dashed) and uncoupled (dotted line) modes. The colored area shows the transmission amplitude defined in Eq. (7).

in oscillator systems having at least weak nonlinear interactions. It was shown experimentally that spin-torque nano-sized oscillators can be phase locked to an external microwave signal [29] as well as two single spin torque nano-oscillators (STNO) in close proximity mutually phase-lock [30]. Locking of collective dynamics occurs due to dynamic exchange coupling between two FMs separated by normal metal, where spin pumping synchronizes two modes [31]. The phase-locked state is distinct, characterized by a sudden narrowing of signal linewidth and an increase in power due to the coherence of the individual oscillators. The physical picture of phase locked coupling in the system is the following: a localized magnetic moment suddenly changes its direction causing a voltage in LCR circuit due to the Faraday induction. This voltage causes a current in the circuit, which, in turn, produces magnetic field due to Ampere's law and exerts torque on the magnetization acting as anti-damping torque.

To calculate the FMR linewidth we solve the Eq. (6) for ω_r. In contrast to the solution for ω here we have only one solution. The real part of the $\omega_r(\omega)$ is the FMR spectrum while the imaginary part is the linewidth $\Delta H = Im(\omega_r(\omega))/Re(\omega_r(\omega))$. It has bees demonstrated that in the coupled cavity FMR system the normalized linewidth is being changed by the coupling [18]. In Fig. 2 (a) we plot the normalized linewidth dependence on ω. In the absence of relative phase shift ($\Phi = 0$) the normalized linewidth is being increased near the resonance by the coupling (solid line in the picture) [18]. Dotted curve shows that in the absence of magnon-photon coupling the linewidth is constant and determined by the damping constant α. However, in the case when $\Phi \approx \pi$ relative phase shift is introduced the linewidth is decreasing (dash-dotted curve in Fig. 2 (a)) near the resonance frequency as it is expected for the phase locked coupling. In order to analyse the second characteristic feature of phase locked coupling, namely the signal power enhancement, we calculate the transmission amplitude using input-output formalism [18, 32]

$$S_{21} = \Gamma \frac{e^{i\Phi}\omega^2 \left(\omega(\alpha - i) + i\omega_r\right)}{\det \Omega}, \tag{7}$$

where $\Gamma \approx 10^{-4}$ characterizes the cavity/cable impedance mismatch. In Fig. 2 (b) we plot the spectrum of the coupled system, where the dashed line is $Re(\omega(\omega_r))$ and the colored area represents the transmission amplitude. It is seen that the transmission amplitude - proportional to transmission power - is lower at FMR frequencies far from resonance and increases dramatically when ω_r approaches to ω_c. Fig. 3 shows the transmission amplitude evolution as a function of ω at different fixed values of FMR frequency ω_r. At FMR frequencies far from resonance, $|\omega_r - \omega_c| > \omega_{g0}$, the transmission amplitude is not affected by the FMR and the transmission is due to the cavity mode and is equal to that of empty cavity. Tuning the FMR frequency close to resonance with the cavity mode, $|\omega_r - \omega_c| \lesssim \omega_{g0}$, the transmission amplitude increases and reaches its maximum (sharp peak in Fig. 3) at resonance $\omega_r = \omega_c$.

In contrast to $\Phi = 0$ discussed in Ref. 18, where the linewidth always increases as the FMR approaches the resonant coupling condition, no matter whether $\alpha < \beta$ or $\alpha > \beta$, here both transmission coefficient and FMR linewidth depend on interplay between damping of two oscillators and coupling strength. For a very small damping and strong coupling the system becomes not stable anymore (for $\Phi \approx \pi$) and the assumption of simple periodic motion leads to negative value of the linewidth in Fig. 2 (a). It is known that the combination of energy injection and dissipation maintains macroscopic systems out of the equilibrium [33]. This can generate complex dynamical states, such as noise-periodicity, intermittency or chaos [34]. We believe that more systematic study of complicated dynamic phases in this regime would be useful by using numerical methods. We define a condition of stability of the system in such a way that the FMR linewidth is positive. At resonant frequency, where $\omega = \omega_c$, this condition

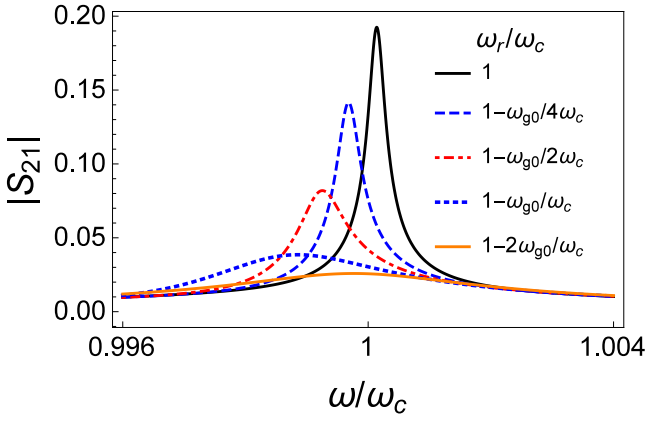

Figure 3. (Color online) Evolution of the transmission amplitude as a function of ω at different fixed values of FMR frequency.

leads to $\alpha\beta = K^2\omega_m/2\omega_c$. Thus, large cavity damping can be compensated by low Gilbert damping.

In summary, we study the magnon-photon coupling in cavity in the presence of relative phase shift between microwave magnetic and electric components. We show that the anti-crossing gap between the hybridized cavity and FMR modes can be controlled by relative phase. Increasing the phase shift leads to reduction of the gap and eventually forming the phase locked spectrum when the relative phase equals to π. At this regime two modes start to beat at almost the same frequency in $|\omega_r - \omega_c| \lesssim \omega_{g,0}$ range. Linewidth drop and power enhancement - that are distinct features of synchronization of coupled oscillators - is demonstrated.

This work was funded by National Natural Science Foundation of China (Grants No. 61376105, 11174037).

* Corresponding author: kexia@bnu.edu.cn

[1] D. L. Mills and E. Burstein, Reports Prog. Phys. 37, 817 (1974).
[2] R. H. Dicke, Phys. Rev. 93, 99 (1954).
[3] M. Tavis and F. W. Cummings, Phys. Rev. 170, 379 (1968).
[4] Y. Kubo, F. R. Ong, P. Bertet, D. Vion, V. Jacques, D. Zheng, A. Dreau, J. F. Roch, A. Auff'eves, F. Jelezko, J. Wrachtrup, M. F. Barthe, P. Bergonzo, and D. Esteve, Phys. Rev. Lett. 105, 140502 (2010).
[5] R.Amsuss, C.Koller, T.Nobauer, S. Putz, S. Rotter, K. Sandner, S. Schneider, M. Schrambock, G. Steinhauser, H. Ritsch, J. Schmiedmayer, and J. Majer, Phys. Rev. Lett. 107, 060502 (2011).
[6] D. I. Schuster, A. P. Sears, E. Ginossar, L. DiCarlo, L. Frunzio, J. J. L. Morton, H. Wu, G. A. D. Briggs, B. B. Buckley, D. D. Awschalom, and R. J. Schoelkopf, Phys. Rev. Lett. 105, 140501 (2010).
[7] S. Probst, H. Rotzinger, S. Wunsch, P. Jung, M. Jerger, M. Siegel, A. V. Ustinov, and P. A. Bushev, Phys. Rev. Lett. 110, 157001 (2013).
[8] K. Sandner, H. Ritsch, R. Amsuss, Ch. Koller, T. Nobauer, S. Putz, J. Schmiedmayer, and J. Majer, Phys. Rev. A 85, 053806 (2012).
[9] H. Huebl, C. W. Zollitsch, J. Lotze, F. Hocke, M. Greifenstein, A. Marx, R. Gross, and S. T. B. Goennenwein, Phys. Rev. Lett. 111, 127003 (2013).
[10] Y. Tabuchi, S. Ishino, T. Ishikawa, R. Yamazaki, K. Usami, and Y. Nakamura, Phys. Rev. Lett. 113, 083603 (2014).
[11] X. Zhang, C.-L. Zou, L. Jiang, and H. X. Tang, Phys. Rev. Lett. 113, 156401 (2014).
[12] N. J. Lambert, J. A. Haigh, S. Langenfeld, A. C. Doherty, and A. J. Ferguson, Phys. Rev. A 93, 021803(R) (2016).
[13] J. J. Viennot, M. C. Dartiailh, A. Cottet, T. Kontos, Science 24, Vol. 349, 408 (2015).
[14] Y. Tabuchi, S. Ishino, A. Noguchi, T. Ishikawa, R. Yamazaki, K. Usami, Y. Nakamura, Science 24, Vol. 349, 405 (2015).
[15] S. Haroche and J.-M. Raimond, Exploring the Quantum: Atoms, Cavities and Photons (Oxford University Press, Oxford, 2006).
[16] A. Blais, R.-S. Huang, A. Wallraff, S. M. Girvin, and R. J. Schoelkopf, Phys. Rev. A 69, 062320 (2004).
[17] A. Wallraff, D. I. Schuster, A. Blais, L. Frunzio, J. Majer, S. Kumar, S. M. Girvin, and R. J. Schoelkopf, Nature (London) 431, 162 (2004).
[18] L. Bai, M. Harder, Y. P. Chen, X. Fan, J. Q. Xiao, and C.-M. Hu, Phys. Rev. Lett. 114, 227201 (2015).
[19] Yunshan Cao, Peng Yan, Hans Huebl, Sebastian T. B. Goennenwein, and Gerrit E. W. Bauer, Phys. Rev. B 91, 094423 (2015).
[20] M. Harder, L. H. Bai, C. Match, J. Sirker, and C. M. Hu, Sci. China-Phys. Mech. Astron. 59, 117511 (2016).
[21] A. Wirthmann, X. Fan, Y. S. Gui, K. Martens, G. Williams, J. Dietrich, G. E. Bridges, and C.-M. Hu, Phys. Rev. Lett. 105, 017202 (2010).
[22] Z. X. Cao, W. Lu, L. Fu, Y. S. Gui, C.-M. Hu, Appl Phys A 111, 329 (2013).
[23] Y. S. Gui, N. Mecking, X. Zhou, G.Williams, and C. -M. Hu, Phys. Rev. Lett. 98, 107602 (2007).
[24] N. Mecking, Y. S. Gui, and C.-M. Hu, Phys. Rev. B 76, 224430(2007).
[25] N. Bloembergen and R. V. Pound, Phys. Rev. 95, 8 (1954).
[26] T. J. Silva, C. S. Lee, T. M. Crawford, and C. T. Rogers, J. Appl. Phys. 85, 7849 (1999).
[27] T. L. Gilbert, IEEE Trans. Magn. 40, 3443 (2004).
[28] L. Bai et al., IEEE Trans. Magn. 52, 1 (2016).
[29] W. H. Rippard, M. R. Pufall, S. Kaka, T. J. Silva, S. E. Russek, and J. A. Katine, Phys. Rev. Lett. 95, 067203 (2005).
[30] S. Kaka, M. R. Pufall, W. H. Rippard, T. J. Silva, S. E. Russek, and J. A. Katine, Nature Vol 437, 15 (2005); Strogatz, S. Sync: The Emerging Science of Spontaneous Order 51, 116 (Hyperion, New York, 2003).; York, R. A., IEEE Trans. Microwave Theory Tech. 41, 1799 (1993).; Rezavi, B., IEEE J. Solid State Circuits 39, 1415 (2004).
[31] Heinrich B., Y. Tserkovnyak, G. Woltersdorf, A. Brataas, R. Urban, and G. E. W. Bauer, Phys. Rev. Lett. 90, 187601 (2003).
[32] M. Harder, P. Hyde, L. Bai, Ch. Match, and C.-M. Hu, Phys. Rev. B 94, 054403 (2016); M. Harder, Z. X. Cao, Y. S. Gui, X. L. Fan, and C.-M. Hu, Phys. Rev. B 84, 054423 (2011).
[33] M.C. Cross, P.C. Hohenberg, Rev. Mod. Phys. 65, 851 (1993).
[34] Z. Li, Y.C. Li, S. Zhang, Phys. Rev. B 74, 054417 (2006); Z. Yang, S. Zhang, and Y. C. Li, Phys. Rev. Lett. 99, 134101 (2007); E.N. Lorenz, J. Atmos. Sci. 20, 130 (1963); C. Sparrow, The Lorenz Equations: Bifurcations, Chaos and Strange Attractors (Springer, New York, 1982); E. Ott, Chaos in Dynamical Systems (Cambridge University Press, Cambridge, 2002).